Journal of Hydroscience and Hydraulic Engineering
Vol. 24, No.1 May, 2006, 145-155

VELOCITY MEASUREMENTS IN A RIVER WITH A SERIES OF GROYNES BY A SHIP-MOUNTED ADCP

By

MUTO Yasunori [1], KITAMURA Koichi[2], BABA Yasuyuki[1] and NAKAGAWA Hajime [1]

[1] Disaster Prevention Research Institute, Kyoto University, Fushimi, Kyoto, Japan
[2] Ishikawajima-Harima Heavy Industries, Co., Ltd., Tokyo, Japan
(Formerly Graduate School Student, Kyoto University)

SYNOPSIS

Velocity measurements were carried out in a river of straight reach with a series of groynes on one side of the main channel. A broadband Acoustic Doppler Current Profiler (ADCP) mounted on a small boat was used. The measurements were performed in the area of 60m times 200m including four groynes, under three depth conditions including two submerged cases during floods. For the non-submerged case, a 2-D large circulation flow is dominant, whereas a complex 3-D flow structure is observed in the submerged cases. The exchange process is also governed by the 2-D circulation in the non-submerged case, whereas a weak depth-scale secondary flow cell is formed in the junction region in the submerged case. Sediment deposition in the embayment is strongly affected by those local flow structures. Patches of vegetations on the bank can well be correlated with the flow dynamics and the resultant sediment movements.

INTRODUCTION

Groynes and spur dykes are primarily used for bank protection and channel stabilisation. In recent years, in addition, these structures have acquired new functions, i.e. the creation and preservation of a good habitat. Groynes disturb water flow, and then cause bed evolution around them. This means that groynes produce a variety of flow velocities and water depth, which improves simple river coast geometry of prismatic channels. Acting in such a manner, groynes can create various ecological conditions for riverine natural lives.

Flow structures around groynes are quite complex. Owing to the existence of the groyne itself, flow diversion occurs and the diverted flow is accelerated. Such acceleration causes severe local scouring around the top of the groyne. On the other hand, a circulating flow is usually induced behind the groyne, in a so-called groyne field. A good portion of the sediments in the main flow is trapped by

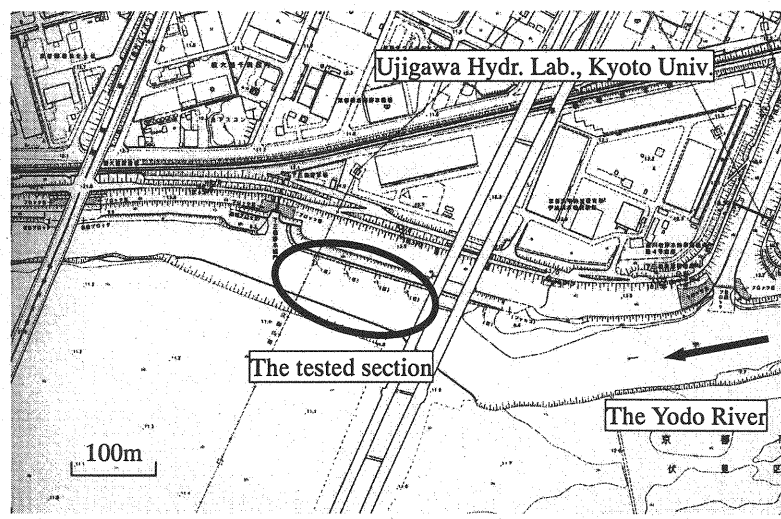

Fig. 1 Location of the tested section.

this circulation, and then is deposited into the groyne field. Such phenomena of the flow and sediment movements in a groyne field have been widely studied experimentally (Fukuoka et al., 1998; Ohmoto et al., 1998; Yossef & de Vriend, 2004). Furthermore, recent advanced numerical models can simulate these processes quite reasonably (Otsuki et al., 2000; Kimura et al., 2004; Zhang et al., 2005). In contrast, field data which verify both experimental results and numerical simulations are quite limited (Muneta et al., 1996). The authors (Fujita et al., 2004) conducted velocity measurements by means of large-scale particle image velocimetry (LSPIV) and showed that several unique features specially seen in the flow around groynes through the measured velocity distributions on the water surface.

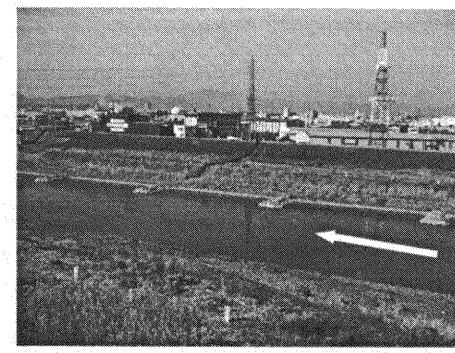

Photo. 1 The tested section.

This study shows velocity distributions and bed topography in the same river reach as the previous study, but also adding measurements under different conditions as well as information on the internal flow structure. The measurements were carried out by using an Acoustic Doppler Current Profiler (ADCP) mounted on a small boat, and conducted under three depth conditions including groynes' submerged cases. The effect of flow pattern and sediment deposition on vegetation along the riverside is also examined.

MEASUREMENT LOCATION AND SET-UP

The test section is on the Yodo River, located about 42.8km from the river mouth, and situated on the south end of Kyoto City. The test section has a compound cross section, whose total width is about 600m, and the main channel width about 60m. The channel bed slope is the order of 10^{-4}. Four rock dykes were constructed only on the righthand side of the main channel along nearly a straight reach. Each dyke extends about 10m perpendicular from the channel side toward the main stream. The

longitudinal distance from one dyke to the next is about 40m. The aspect ratio of the embayments is 4 (see Fig. 1 and Photo. 1). Figure 2 shows a schematic view of the tested area, together with the definition of the coordinate system.

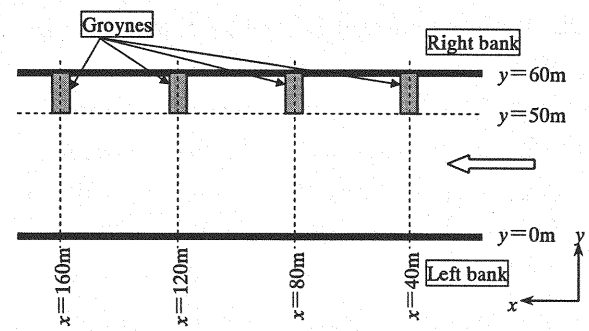

Fig. 2 Schematic view of the tested section and the definition of the coordinate system.

A 4-beam broadband Acoustic Doppler Current Profiler (ADCP), Workhorse Sentinel 1200ZB, RD Instruments, USA, was used for the velocity measurements. The ADCP was mounted on a small boat with a 5 hp engine. Velocity data were obtained by driving the boat in the longitudinal direction. While driving downstream, the engine was kept at minimum power and only the rudder was used to maintain the direction and the position of the boat, whereas while driving upstream the speed of the boat was kept at less than 1kt. In the main channel, the transverse distance of each driving path was set at less than 10m, and 6 paths were drawn in the 50m wide. This measurement procedure was repeated more than 10 times, which yields the averaged distance of the driving path of about 1m. In the groyne fields, whose area of 40m×10m each, more than 10 longitudinal driving paths were drawn, which also yields the averaged distance of the driving path of about 1m. The position information on the measuring point was given by the bottom tracking system working together with the ADCP. In addition, a differential Global Positioning System (D-GPS) was also used as a reference. The ADCP was operated in the high-speed pinging mode, i.e. pinging was emitted at 25Hz and 20 data were averaged for one measurement. The averaged data were obtained every 1.1 seconds, including time allotted for calculation. Spatial resolution of the measurement points along the driving path depends on the boat speed and the flow velocity, and was about 1m in average. Eventually 1m×1m measurements grids were drawn in the tested area of 200m ×60m including groyne fields. Resolution in the vertical direction was set at 25cm.

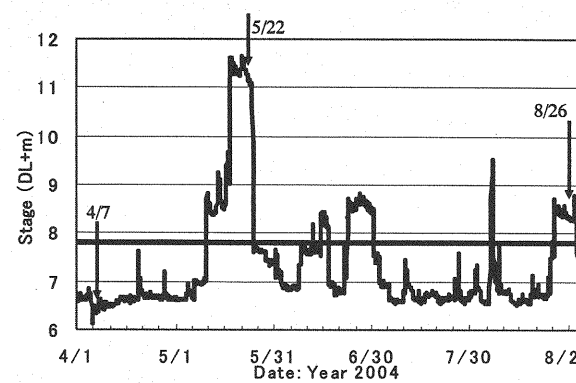

Fig. 3 Variation of the stage at the tested section from April to August, 2004.

The flow discharge in the tested section is fully controlled by a high dam located 10km upstream. Figure 3 shows an hourly variation of the stage at the tested section from April to August, 2004, together with the level of the groyne head. The measurements were carried out three times during that period, April 7th, May 22nd and August 26th. As can be seen from the figure, the depth condition in April was non-submerged one, whereas in May and in August being under submerged conditions. The averaged flow discharge in the tested section given by the Ministry of Land Infrastructure and Transport, Japan was ca.75m^3/s, 780m^3/s and 330m^3/s respectively. The Reynolds

number is the order of 10^6 and the Froude number is 0.15 to 0.35.

Table 1 shows comparisons between the calculated discharge by integrating the velocity distributions measured by the ADCP and the actual discharge. It is shown that the ADCP gives quite precise values, hence the applicability of the measurement procedure can be confirmed.

Figure 4 shows the bed shape of the tested section measured by the ADCP. Judging from the figure, it can be said that the channel geometry do not change so much from April, the top, to August, the bottom, although several floods occurred during that time (see Fig. 3).

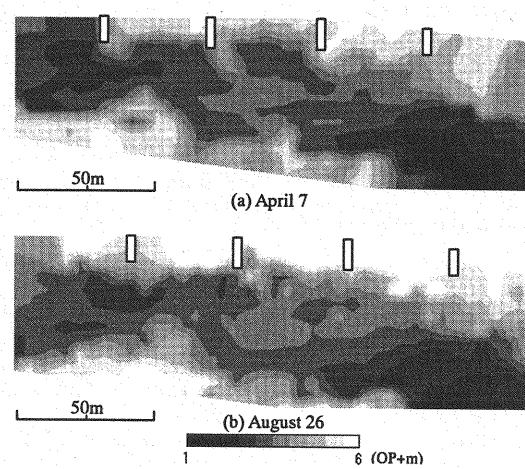

Fig. 4 Bed shape of the tested section.

Table 1 Comparisons between the actual discharge and the calculated discharge. (unit: m^3/s)

	Actual Q	Measured Q
Apr. 7	75	75 - 80
May 22	780	730 - 750
Aug. 26	330	330 - 340

RESULTS AND DISCUSSIONS

Velocity Distributions in the Groyne Fields

Figures 5 to 7 show velocity distributions in the tested area in a plan view. Here the data are spatially averaged in the grid size of 5m×5m by using the raw data on the aforementioned 1m×1m grid. In the figures, the resultant velocity is plotted as a vector form, together superimposed the longitudinal velocity as a contour form.

In Fig. 5, the non-submerged case, one can see that the longitudinal velocity is negative in most of the groyne fields. There forms a steep velocity gradient between the main channel and the groyne fields. From the vector plotting, it seems that a large clockwise circulation is formed in each groyne field. These flow patterns can be seen both

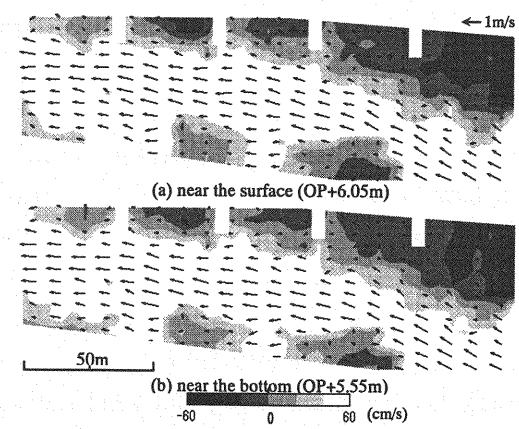

Fig. 5 Velocity distributions in the non-submerged case, April 7.

near the water surface and near the bottom, thus it can be recognised that flow structure in the groyne field is 2-D.

Figure 6 shows the shallow submerged case, where the overtopping depth was about 60cm. In this case, adverse flow regions shrink, but the 1st embayment and its upstream region are still negative. In the 2nd and 3rd embayments, flow near the water surface runs downstream, but in contrast upstream near the bottom, which indicates that vertical circulation is induced in the groyne field.

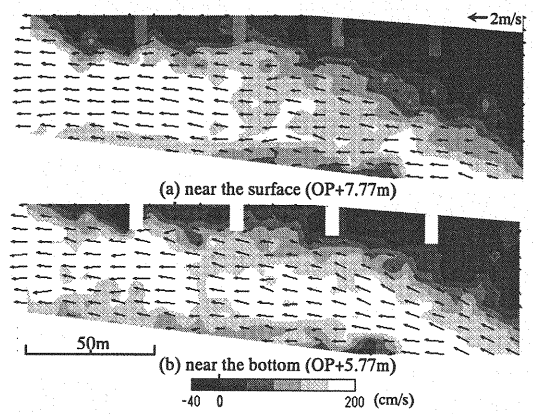

Fig. 6 Velocity distributions in the shallow submerged case, August 26.

The results for the deep submerged case are shown in Fig. 7. At that time, the overtopping depth was about 3.5m. It can be seen from the figure that adverse flow regions nearly disappear, except for a quite limited area just behind the groynes. An area upstream of the 1st groyne also shows negative values, which can be influenced by a sand bar formed upstream of the tested section (see Fig. 1).

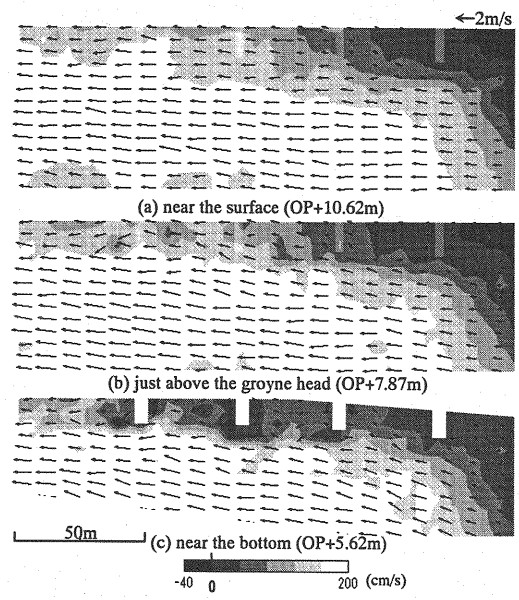

Fig. 7 Velocity distributions in the deep submerged case, May 22.

Transverse Distributions of the Longitudinal Velocity in the Main Flow Region

In a previous paper (Fujita et al., 2004), the authors pointed out that the maximum velocity filament shifted considerably toward the river bank opposite to the groynes' side. Here the internal structure of the shifting is examined.

Figure 8 shows transverse distributions of the longitudinal velocity near the water surface in several sections between the 2nd and 4th groynes (see Fig. 2). For the non-submerged case the maximum velocity appears at around y=25m, which can be recognised as the centre of the channel excluding the groyne field. On the other hand, the maximum velocity appears at around y=15m for the shallow submerged case, and for the deep submerged case around y=20m. The reason why the shifting is most enhanced in the shallower case could be attributed to the role of the groyne fields in the channel conveyance capacity. That is, for the shallow submerged case the velocity in the groyne fields is as small as for the non-submerged case, hence flow in the main channel, especially on the groyne side, is retarded severely. Whereas for the deep submerged case, the groyne fields bear discharge to some degree, although the groynes still work as an extensive roughness factor. In addition, the upstream sand bar (see Fig. 1) could also influence the velocity shifting, since it changes its appearance from the non-submerged condition to the

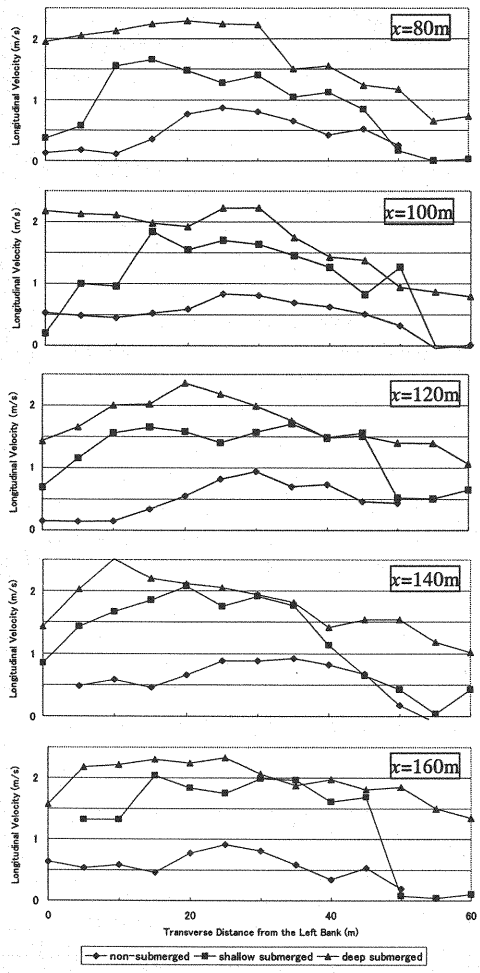

Fig. 8 Transverse distributions of the longitudinal velocity near the water surface.

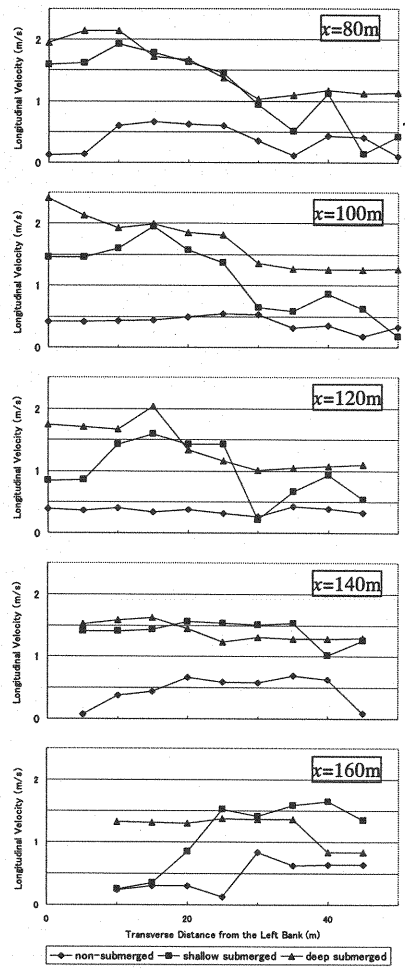

Fig. 9 Transverse distributions of the longitudinal velocity near the river bed.

submerged one according to the depth in the range studied here.

Figure 9 shows the velocity distributions near the channel bottom in the same manner as Fig. 8. It can be said that in the sections x=120m and upstream the position of the maximum velocity well coincides with that seen near the water surface. In contrast, the distributions are nearly uniform at x=140m, then the maximum velocity appears on the opposite side to what is observed near the water surface at x=160m. This can be brought by a mound on the left side of the main channel at around x=150m (see Fig. 4). This mound considerably reduces the width of the channel near the bottom, hence the velocity distributions are much distorted there.

Consequently, in the tested section the maximum velocity filament appears more or less the same position on the water surface and near the bottom, which means the flow in the main channel is so-called 2-D, except the area where a local effect such as a mound is apparent.

Exchange Processes between the Main Channel and Groyne Fields

Figures 10 to 12 show cross sectional velocity distributions in order to study exchange processes between the main channel and groyne fields. Here the longitudinal velocity is shown in a contour form, and the secondary flow is plotted as a vector form.

Figure 10 shows the results for the non-submerged case. The junction between the main channel and the groyne field is indicated by a black solid line. At x=155m, 5m upstream of the 4th groyne, the flow in the embayment goes from the junction toward the river bank, whereas at x=125m, 5m downstream of the 3rd groyne, the dominant flow direction in the embayment is opposite. In the central part, x=140m, the transverse velocity at the junction is quite small compared with the other two sections. The flow pattern described here well coincides with what is seen in Fig. 5, i.e. the horizontal circulation induced in the embayment. Therefore, the flow exchange in this case is active near the groynes, but not so much in the central part of the groyne field.

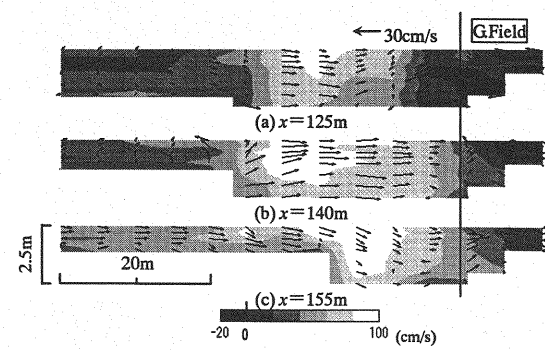

Fig. 10 Cross sectional velocity distributions in the non-submerged case, April 7.

Figure 11 shows the results for the deep submerged case. At the section x=120m, where is the position of the 3rd groyne, the flow from the main channel to the embayment is dominant. Whereas in the following two sections, returning currents from the embayment to the main channel can be seen near the bottom. This could be a weak clockwise cell-like structure. The exchange process in the submerged case can be affected by this cell-like structure, thus it is totally different from that in the non-submerged case.

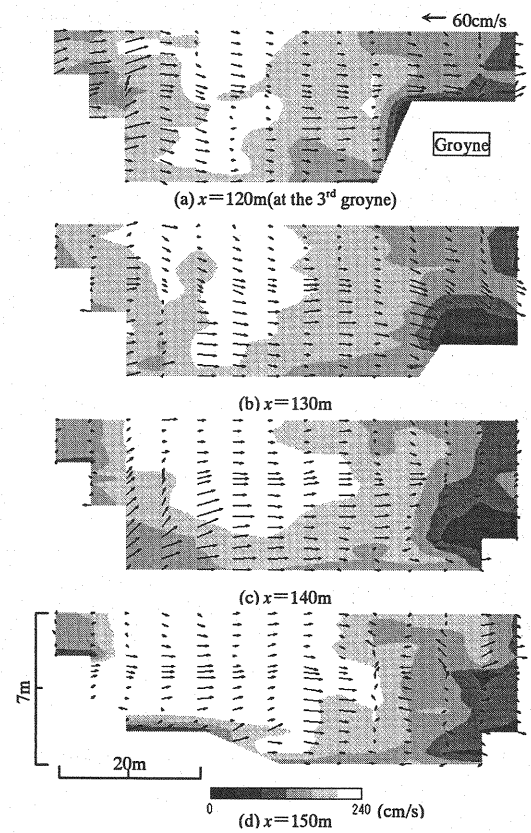

Fig. 11 Cross sectional velocity distributions in the deep submerged case, May 22.

Figure 12 shows cross sectional velocity distributions in the downstream area of the 4th groyne. The aforementioned cell-like motion is much clearer in this figure. It should also be noted that a slow water body around the groyne is trapped by the cell and driven towards the water surface. The estimated point where this water body reaches at the surface almost coincides with the point where the authors observed boils (Fujita et al., 2004). The distance from the groyne to this point estimated by

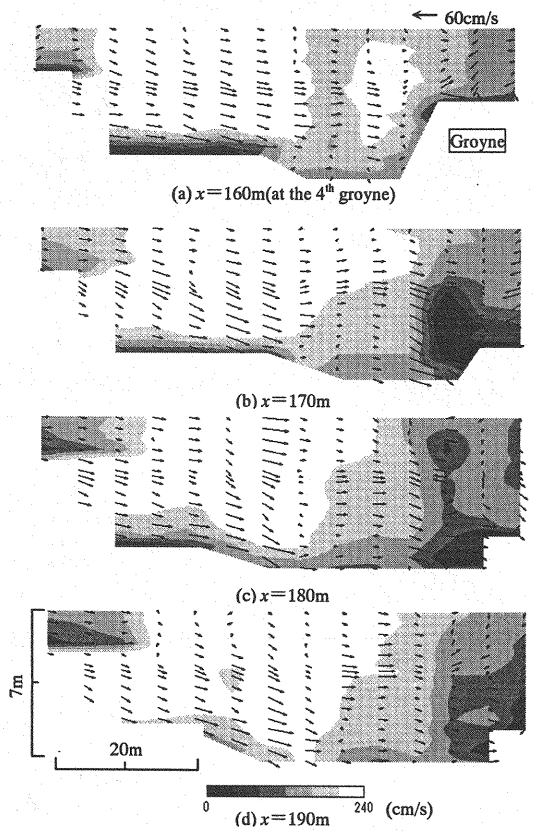

Fig. 12 Cross sectional velocity distributions in the deep submerged case, May 22.

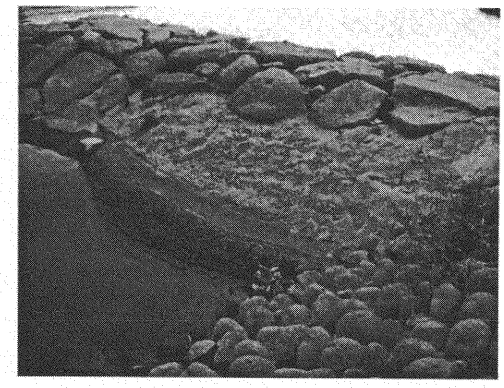

Photo. 2 Deposited sediments at the corner of the groyne field.

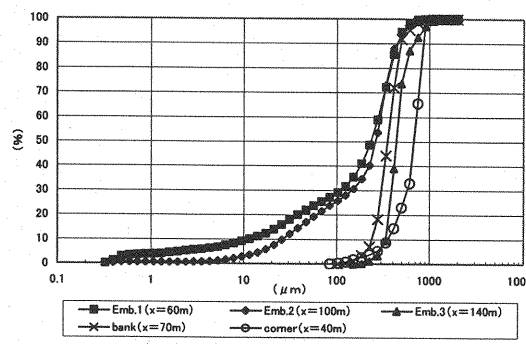

Fig. 13 Grain size distributions.

Fig. 12, and also confirmed in the field, is about 25m. The averaged longitudinal velocity in this area is about 2m/s, reading from Fig. 7. Hence, the travelling time of the body from the groyne to the surface can be calculated as about 12sec. On the other hand, the vertical distance from the groyne to the surface is about 3.5m, therefore the travelling velocity in the vertical direction is about 30cm/s. This value is nearly twice the averaged vertical velocity observed in the figure. Further study is necessary to clarify the behaviour of the slow water body and the boil, since it can have a significant influence on the sediment movements in the groyne field.

Sediments and Vegetation Characteristics

As already shown in Fig. 4, the bed shape of the tested section is not so much changed from April to August. In contrast, sediment depositions are apparent at the corner of the groyne field (see Photo. 2), and on the river bank. Grain size distributions of these deposited sediments were analysed, together with those from the bottom of the embayments, and are plotted in Fig. 13. It can be seen from the figure that the mean diameter of the sediments is nearly the same irrespective of the collecting point, 0.2 to 0.8mm, which is 2 orders smaller than that collecting at the bottom of the main channel, 2 to 4cm (CTI Engineering Co., Ltd., 2001; Foundation of River & Watershed Environment Management, 2004). It should also be noted that the sediments from the bottom of the embayments

Photo. 3 Vegetation distributions on the slope of the river bank.

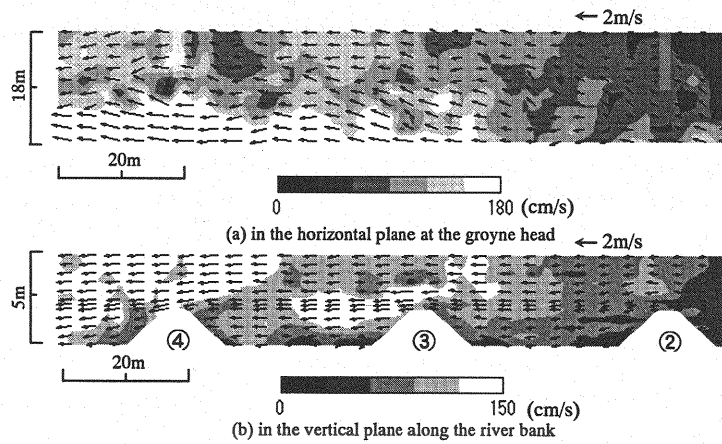

Fig. 14 Velocity distributions in the 2nd and 3rd embayments in the submerged case, May 22.

contain larger portions of fine materials whose diameter is less than 0.1mm than those on the bank. In addition, the 1st embayment has the largest portion, and that portion decreases as goes downstream. Such spatial variation of sediment distribution within a series of groyne fields is quite important when considering physical basics for microhabitat.

Photograph 3 shows patches of vegetation on the slope and path of the river bank. These surfaces were originally covered by stone-like concrete blocks, which help trapping sediments in their porous spaces, and eventually allow vegetation grow. In the photograph, however, one can notice that in some parts well flourish but not in others. Within one embayment, vegetation flourishes more in the downstream half than the upstream. Such spatial difference on the growth of the vegetation can be explained by the local flow structure shown in Fig. 14. The figure shows velocity distributions in the 2nd and 3rd embayments more closely. In a horizontal plane at the height of the groyne head, (a), flow from the embayment onto the bank is clearly detected especially in the downstream half. On the other hand, in a vertical plane along the river bank, (b), a faster flow and a slower flow appears alternatively at around the groyne head level, and the slower flow is mainly seen in the downstream half. It can therefore be concluded that under the flooding conditions flow onto the bank is more active in the downstream half of an embayment, and this flow brings and deposits sediments when its velocity is retarded on a shallower bank area, which will lead to settle more vegetation when the water stage falls after the flooding event.

CONCLUSIONS

- Velocity measurements were carried out in a river of straight reach with a series of groynes using an ship-mounted Acoustic Doppler Current Profiler (ADCP). Accuracy of the measurements was verified by checking the integrated discharge given by the ADCP, and was confirmed in the errors in the estimated discharge of mostly less than 5%.
- The effect of depth dependency on the flow dynamics in the groyne fields can be summarised as the structure of circulating flow. That is, in the non-submerged case a horizontal circulation is dominant, whereas when the groyne is submerged a vertical circulation is formed behind the groyne and the horizontal circulation cannot be seen. When the water depth much increases, however, the size of the vertical circulation becomes quite small and nearly the whole area runs downstream.
- Owing to the existence of the groynes the transverse distributions of the longitudinal velocity are distorted. The maximum velocity filament is shifted toward the side apart from the groynes. The filament appears more or less in the same position on the water surface and near the bottom, except for the area where a local effect such as a mound is apparent.
- Exchange processes between the main channel and the groyne fields also show the effects of depth dependency. In the submerged case, a weak secondary flow cell is formed in the junction region, and its developing and decaying processes is deemed to have strong influence on the exchange processes. This cell has also close relationship with boils, capturing slow water body around the groyne and driving it to the water surface.
- In and around the groyne fields fine sediments are deposited whose mean diameter is 2 orders smaller than that in the main channel. A good portion of the deposited sediments in the embayments is wash load whose diameter is less than 0.1mm, and this ratio varies from one embayment to another. Sediment deposition in one embayment is strongly affected by the local flow structure especially around the groyne and the river bank. Patches of vegetations on the bank can therefore be clearly explained by the flow dynamics and the resultant sediment movements.
- A weak point of the measurements technique adopted here is relatively short estimating time for each measurements point. Nevertheless, as for the mean structures such as the longitudinal velocity in the main channel and a large-scale circulation in the groyne fields, the technique is shown to yield reliable results to some extent. On the other hand, it should also be noted that this technique does not give information on an instantaneous flow field. Thus, further confirmation will be necessary to determine whether motions like a boil and a secondary flow cell can really be detected by this technique, even though the results shown here agree well with those drawn from a flow visualisation technique.

ACKNOWLEDGEMENTS

The authors would like to appreciate the financial support of Foundation of River & Watershed Environment Management, Japan, headed by Prof. MURAMOTO, Y., Grant-in Aid for Scientific Research (A)(2), JSPS, Japan, headed by Prof. IKEBUCHI, S. and Grant-in Aid for

Scientific Research (B)(2), JSPS, Japan, headed by the forth author. The authors would also say thanks to Prof. AYA, S., Osaka Institute of Technology, and Prof. FUJITA, I., Kobe University, for their encouragement and comments on the paper.

REFERENCES

CTI Engineering Co., Ltd. : Report on a river development plan of the Yodo River, 2001. (in Japanese)

Foundation of River & Watershed Environment Management : Report on a construction plan of navigation passage in the Yodo River, 2004. (in Japanese)

Fujita, I., Muto, Y., Shimazu, Y., Tsubaki, R. and Aya, S. : Velocity measurements around non-submerged and submerged spur dykes by means of large-scale particle image velocimetry, J. Hydroscience and Hydraulic Engineering, Vol.23, No.1, pp.51-61, 2004.

Fukuoka, S., Nishimura, T., Okanobu, M. and Kawaguchi, H. : Flow and bed topography around groins installed in a straight channel, Annual J. of Hydraulic Engineering, JSCE, Vol.42, pp.997-1002, 1998. (in Japanese)

Kimura, I., Hosoda, T., Onda, S. and Tominaga, A. : Computations of 3D turbulent flow structures around submerged spur dikes under various hydraulic conditions, River Flow 2004, Naples, Italy, 2004.

Muneta, N., Shimizu, Y. and Itakura, T. : About grain size distribution and river bed change around a spur-dyke with a flood, Annual J. of Hydraulic Engineering, JSCE, Vol.40, pp.799-804, 1996. (in Japanese)

Ohmoto, T., Hirakawa, R. and Ide, K. : Responses of secondary currents and sediments to submerged groynes, Annual J. of Hydraulic Engineering, JSCE, Vol.42, pp.1003-1008, 1998. (in Japanese)

Otsuki, H., Ashida, K., Abe, S., Wada, H. and Fujita, A. : Hydraulic performance of groins and their effects of the bank and bed protection, J. of Hydraulic, Coastal and Environmental Engineering, JSCE, No.663/II-53, pp.11-30, 2000. (in Japanese)

Yossef, M.F.M. and de Vriend, H.J. : Mobile-bed experiments on the exchange of sediment between main channel and groyne fields, River Flow 2004, Naples, Italy, 2004.

Zhang, H., Nakagawa, H., Ishigaki, T. and Muto, Y. : Prediction of 3D flow field and local scouring around spur dykes, Annual J. of Hydraulic Engineering, JSCE, Vol.49, pp.1003-1008, 2005.

APPENDIX – NOTATION

The following symbols are used in this paper:

Q = discharge;

x = longitudinal distance; and

y = transverse distance.

(Received October 17, 2005 ; revised January 10, 2006)